한국해양공학회 2002년도 추계학술대회 논문집 PP.212~216

Simulation of Viscous Flow around a Circular Cylinder between Parallel Walls

SEUNG-HYUN KWAG
School of Mechanical Engineering, Halla University, Wonju 220-712, Korea

KEY WORDS: Viscous Flow 점성유동, Circular Cylinder 원형실린더, Navier-Stokes 나비에-스톡스, Third Derivative Upwind, 3차풍상미분, Numerical Simulation 수치재연

ABSTRACT: *평행한 벽 내부의 흐르는 유체 속에 원형실린더를 놓고 유동장 해석을 수행하였다. 비압축성 Navier- Stokes 방정식을 풀었고 3차 풍상미분의 수치해법을 이용하였다. 채널 내부에서 실린더의 위치를 이동하면서 벽면의 효과, 전단력, 와류의 현상을 규명하였다. 수치처리는 Marker & Cell 기법에 의한 유한차분법을 사용하였다. 본 연구를 통하여 실린더와 벽 경계 사이에서의 생성된 와가 박리 전단에 영향을 미치는 것을 알 수 있었다.*

1. INTRODUCTION

The present study is focused on the interaction between a stream in a plane channel and a small circular cylinder placed in it. The flow of an oscillatory stream has received much attention because of its relevance to marine pipelines. The wake structure and related actions on the body have been systematically studied in recently years (Tatsuno & Bearman 1990, Justensen 1991, Chen et. al 1995, Sumer et. al 1991, and Zavatto et. al 2001). The shedding regimes are influenced by the presence of the wall at distances comparable with the cylinder diameter. When the distance is small enough, the vortex shedding is almost completely suppressed because of the interaction with the wall boundary layer separation. In the present study, the Navier-Stokes equations are solved by a finite difference method with a Marker & Cell method such that the continuity equation is exactly satisfied. The results are pertinent only for values of Reynolds number low enough to guarantee the stability of the flows to the disturbances of a channel flow with an immersed body. The reliability depends on whether the combined dynamics would be expected to enhance or reduce the stability of the flow.

This work aims to address questions regarding the characteristics of the vortex shedding regime and its modifications, either qualitatively and quantitatively, as the body approaches one wall as Reynolds number varies in the range from the transition to the periodic shedding regime. The features of the separated vorticity dynamics are analysed at different conditions with particular attention to the interaction between the cylinder wake and the induced separation on the plane walls.

제1저자 곽승현 연락처: 원주시 흥업면 흥업리 산66번지
033-760-1233 shkwag@hit.halla.ac.kr

2. NUMERICAL SCHEME

2.1 Basic equations

Numerical simulations are carried out by solving Navier-Stokes equations. The velocity components u, v and w at (n+1) time step are determined by

$$\begin{aligned} u^{n+1} &= \left(F^n - \Phi_x^n \right) \triangle t \\ v^{n+1} &= \left(G^n - \Phi_y^n \right) \triangle t \\ w^{n+1} &= \left(H^n - \Phi_z^n \right) \triangle t \end{aligned} \tag{1}$$

where

$$F^n = \frac{u^n}{\triangle t} + \left(\frac{1}{Re} + \upsilon_t \right) \nabla^2 u - \left(u^n \frac{\partial u}{\partial x} + v^n \frac{\partial u}{\partial y} + w^n \frac{\partial u}{\partial z} \right)$$

$$-\frac{\partial}{\partial x}\left\{ v_t\left(2\frac{\partial u}{\partial x}\right)\right\}-\frac{\partial}{\partial y}\left\{ v_t\left(\frac{\partial u}{\partial y}+\frac{\partial v}{\partial x}\right)\right\}$$
$$-\frac{\partial}{\partial z}\left\{ v_t\left(\frac{\partial u}{\partial z}+\frac{\partial w}{\partial x}\right)\right\}$$

$$G^n=\frac{v^n}{\triangle t}+\left(\frac{1}{Re}+v_t\right)\nabla^2 v$$
$$-\left(u^n\frac{\partial v}{\partial x}+v^n\frac{\partial v}{\partial y}+w^n\frac{\partial v}{\partial z}\right)$$
$$-\frac{\partial}{\partial x}\left\{ v_t\left(\frac{\partial u}{\partial y}+\frac{\partial v}{\partial x}\right)\right\}-\frac{\partial}{\partial y}\left\{ v_t\left(2\frac{\partial v}{\partial y}\right)\right\}$$
$$-\frac{\partial}{\partial z}\left\{ v_t\left(\frac{\partial v}{\partial z}+\frac{\partial w}{\partial y}\right)\right\} \quad (2)$$

$$H^n=\frac{w^n}{\triangle t}+\left(\frac{1}{Re}+v_t\right)\nabla^2 w$$
$$-\left(u^n\frac{\partial w}{\partial x}+v^n\frac{\partial w}{\partial y}+w^n\frac{\partial w}{\partial z}\right)$$
$$-\frac{\partial}{\partial x}\left\{ v_t\left(\frac{\partial u}{\partial z}+\frac{\partial w}{\partial x}\right)\right\}-\frac{\partial}{\partial y}\left\{ v_t\left(\frac{\partial v}{\partial z}+\frac{\partial w}{\partial y}\right)\right\}$$
$$-\frac{\partial}{\partial z}\left\{ v_t\left(2\frac{\partial w}{\partial z}\right)\right\}$$

and

$$\Phi^n=p+\frac{z}{Fn^2} \quad (3)$$

$$\nabla^2=\frac{\partial}{\partial x^2}+\frac{\partial}{\partial y^2}+\frac{\partial}{\partial z^2} \quad (4)$$

Differentiating Eq. (1) with respect to x, y and z, we can get

$$\nabla^2\Phi=F_x+G_y+H_z$$
$$-(u_x^{n+1}+v_y^{n+1}+w_z^{n+1})/\triangle t \quad (5)$$

The last term in Eq. (5) is expected to be zero to satisfy the continuity condition. Equation (5) can be solved by the relaxation method.

It is desirable to introduce coordinate transformations which simplify the computational domain in the transformed domain

$$\xi=\xi(x,y,z),\ \eta=\eta(x,y,z),\ \zeta=\zeta(x,y,z) \quad (6)$$

Through transformations, Eq. (1) can be written,

$$q_t+Uq_\xi+Vq_\eta+Wq_\zeta$$
$$=\left(\frac{1}{Re}+v_t\right)\nabla^2 q-K-REYSF(\xi,\eta,\zeta) \quad (7)$$

where U, V and W are the contravariant velocities and K is the pressure gradient. The pressure is calculated by the following relaxation formula,

$$\Phi^{m+1}=\Phi^m+\omega\cdot(\Phi^{m+1}-\Phi^m) \quad (8)$$

where (m+1) denotes the next time step and ω is a relaxation factor.

2.2 Computational procedure and boundary conditions

The N-S and Poisson equations are solved after transformation, in which the calculation proceeds through a sequence of loops each advancing the entire flow configuration through sufficiently small finite time increment. The output of each loop is taken as an initial condition for the next. The computation is performed until the state is steady. An Euler explicit scheme is used for the time marching procedure. Pressures are obtained throughout the fluid domain by solving the Poisson equation. Iterations are automatically stopped when the pressure difference between two consecutive approximations is smaller than a certain quantity ε, chosen a priori. The new pressure field generates a new velocity field. The velocity component is updated by using the time-forward difference form of the momentum equations.

The third order upstream difference is used for convection terms with the fourth-order truncation error, for example;

$$U\cdot(\delta f/\delta x)_{i,j,k}$$
$$=U_{i,j,k}\cdot(f_{i-2,j,k}-8f_{i-1,j,k}+8f_{i+1,j,k}$$
$$-f_{i+2,j,k})/12+|U_{i,j,k}|\cdot(f_{i-2,j,k}-4f_{i-1,j,k}$$
$$+6f_{i,j,k}-4f_{i+1,j,k}+f_{i+2,j,k})/4 \quad (9)$$

As boundary conditions, the followings are used.

upstream

$$u(z)=6\times(0.25-(z+h)\times 2)\ ;\ \textit{Poiseuille Profile}$$
$$v=0, w=0 \text{ and } p=0$$
$$\triangle u=\triangle v=\triangle w=0 \quad (10)$$

downstream

$$u\xi=v\xi=w\xi=0$$
$$\triangle u\xi=\triangle v\xi=\triangle w\xi=\triangle p\xi=0 \quad (11)$$

body and wall surfaces

$$u=v=w=0, p\zeta=0$$

$$\triangle u=\triangle v=\triangle w=0, \triangle p\zeta=0 \quad (12)$$

3. RESULTS AND DISCUSSION

The flows around a circular cylinder was numerically tested at different positions; h/H=0.5, 0.65, 0.75. Fig. 1(a) shows the grid view where the grid size is 122x14x58. The close-up view of grid is shown in Fig. 1(b). The time increment $\triangle t$ is 0.0005 to meet the Courant condition.

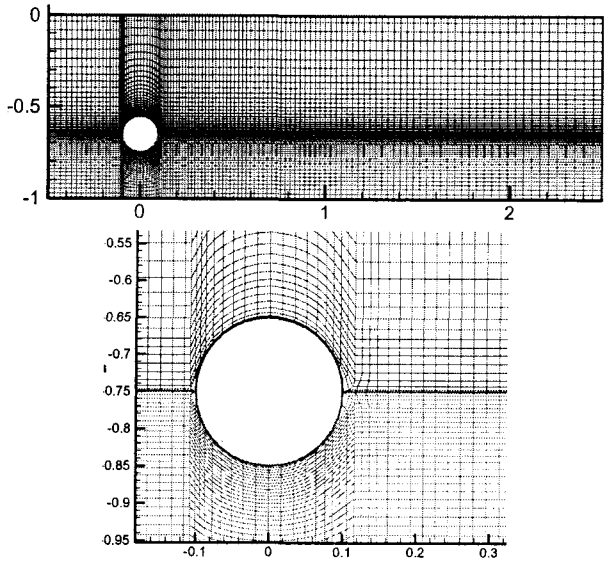

Fig. 1 Grid view around a cylinder body

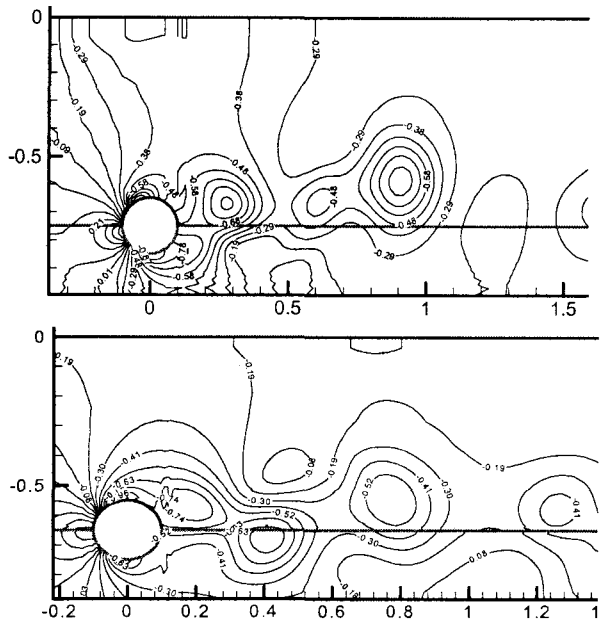

Fig. 2 Pressure contours at h/H= 0.65, 0.75 from above)

For the computation domain, approximately 10 times the cylinder diameter is occupied in downstream and several times in the vertical direction. The grid is made as H-H topology, for the further research, to treat the free surface movement more conveniently. The pressure contours are shown in Fig. 2 at two different positions.

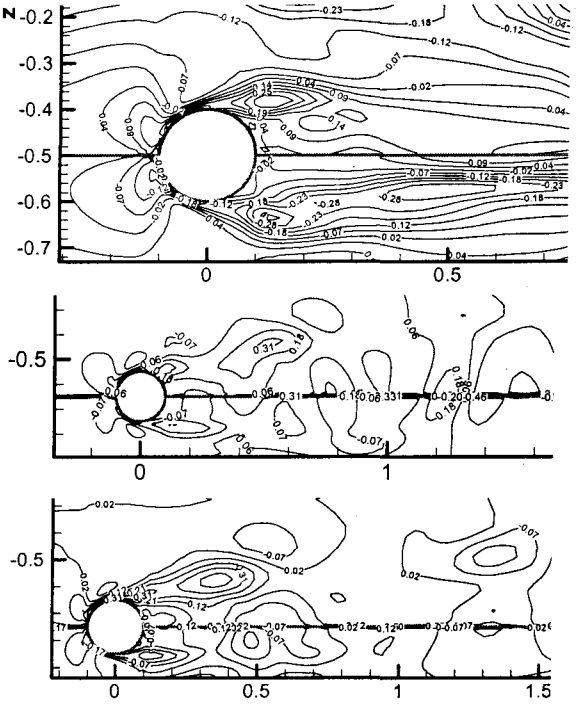

Fig. 3 Vorticity distribution at h/H=0.50, 0.65, 0.75 from above

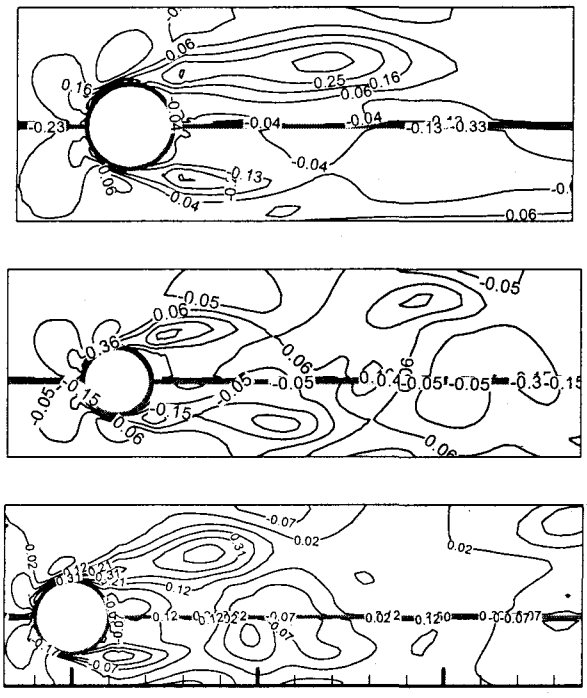

Fig. 4 Vorticity contours at h/H=0.65 (t=2.0, 2.5 and 3.0 from above)

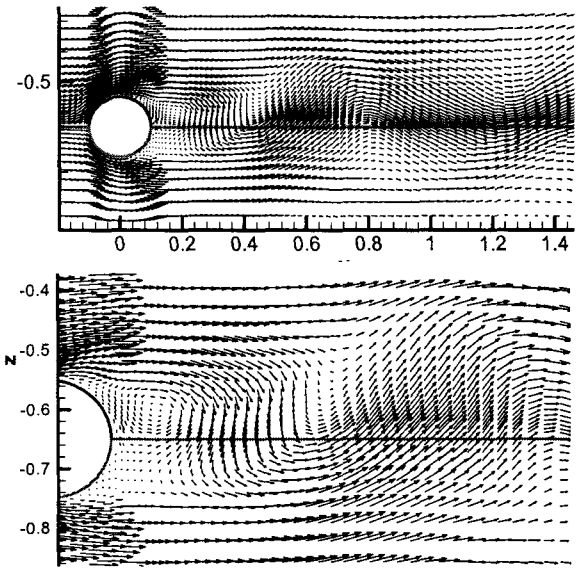

Fig. 5 (a) Close-up view of velocity at h/H=0.65

In Fig. 3, the vorticity contour can be seen around a cylinder at h/H=0.50, 0.65 & 0.75. When the cylinder is placed in the center of the channel, the wake is symmetric and resembles the unbounded case. As the cylinder approaches one wall, the wake vorticity on the wall side is significantly reduced in length. On the opposite face of cylinder the wake elongates, smooths out and eventually combines with the oncoming velocity of the Poiseuille profile. Decreasing the gap value, the wall-side wake couples with the wall boundary layer vorticity of opposite sign while the actual wake is dominated by the vorticity shed from the other side of the body. Fig. 4 shows the vorticity along the non-dimensional marching time of t=2.0, 2.5 and 3.0 for h/H=0.65.

Fig. 5 shows the velocity vectors in the whole domain and close-up view. The different local velocity does not explain the increase of the critical Reynolds number as the cylinder approaches one wall. Neither can an explanation be found in the local irrotational acceleration which occurs only on one side of the body and is reduced on the opposite side. As the body approaches one wall, a local acceleration and deceleration occur on the wall itself; this produces higher vorticity values in the wall boundary layer, and the boundary layer then rapidly grows downstream and influences the cylinder wake on the side facing the wall.

Fig. 6 shows the drag coefficients acting on the cylinder as a function of submerged depth. As can be seen, the solution is close to the steady state after the body has moved about three times of body lengths. The present output was compared with Zovatta's numerical results.

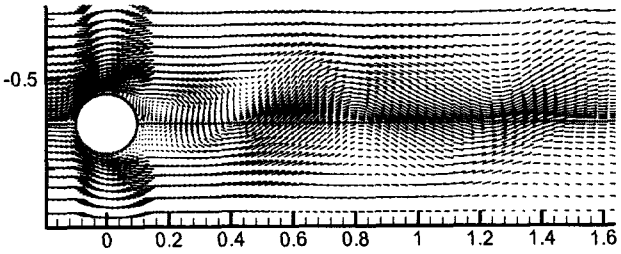

Fig. 5 (b) Velocity vectors at h/H=0.65

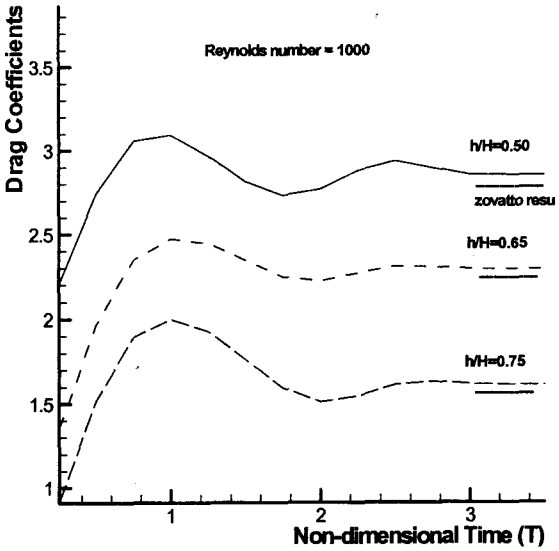

Fig. 6 Drag coefficients along the marching time

4. CONCLUSION

Flows about a circular cylinder placed between two parallel walls are numerically studied at various distances from the wall. The close proximity of one wall exhibits the appearance of vortex shedding. The vortex occurs behind a cylinder when the distance from the wall is small enough. When the cylinder is closer to one wall, the two layers of opposite sign vorticity separated from the cylinder and from the wall, form a pair of vortex sheets which dissipates during the mutually induced stretching. Drag coefficients are predicted along the marching time for the respective depth in which the steady state is obtained around the non-dimensional time of t=3.0.

References

Chen, J. H., Pritchard, W.G., Tavener, S.J. (1995), "Bifurcation for a flow past a cylinder between parallel planes", J.Fluid Mech., Vol. 284, pp. 23-41.

Justensen, P. (1991), "A Numerical Study of Oscillating Flow

around a Circular Cylinder", J. Fluid Mech., Vol. 222, pp.157-196.

Sumer, B. M., Jensen, B. L., Fredsoe, J. (1991), "Effect of a plane boundary on oscillatory flow around a circular cylinder", J.Fluid Mech., Vol. 225, pp. 271-300.

Tatsuno, M., Bearman, P. W. (1990), "A Visual Study of the Flow around an Oscillating Circular Cylinder at Low Keulegan-Carpenter Numbers and Low Stokes Numbers", J. Fluid Mech., Vol. 211, pp. 157-182.

Zovatto, L., Pedrizzetti, G. (2001), "Flow about a circular cylinder between parallel walls", J. Fluid Mech., Vol. 440, pp. 1-25.